

# The output voltage model and experiment of magnetostrictive displacement sensor based on Weidemann effect

Bowen Wang, Yuanyuan Li, Xinliang Xie, Wenmei Huang, Ling Weng, and Changgeng Zhang

Citation: [AIP Advances](#) **8**, 056611 (2018);

View online: <https://doi.org/10.1063/1.5006418>

View Table of Contents: <http://aip.scitation.org/toc/adv/8/5>

Published by the [American Institute of Physics](#)

---

---

## HAVE YOU HEARD?

Employers hiring scientists and  
engineers trust

**PHYSICS TODAY | JOBS**

[www.physicstoday.org/jobs](http://www.physicstoday.org/jobs)



# The output voltage model and experiment of magnetostrictive displacement sensor based on Wiedemann effect

Bowen Wang, Yuanyuan Li,<sup>a</sup> Xinliang Xie, Wenmei Huang, Ling Weng, and Changgeng Zhang

State Key Laboratory of Reliability and Intelligence of Electrical Equipment, Hebei University of Technology, Tianjin 300130, China

(Presented 8 November 2017; received 25 September 2017; accepted 28 October 2017; published online 14 December 2017)

Based on the Wiedemann effect and inverse magnetostrictive effect, the output voltage model of a magnetostrictive displacement sensor has been established. The output voltage of the magnetostrictive displacement sensor is calculated in different magnetic fields. It is found that the calculating result is in an agreement with the experimental one. The theoretical and experimental results show that the output voltage of the displacement sensor is linearly related to the magnetostrictive differences,  $(\lambda_l - \lambda_t)$ , of waveguide wires. The measured output voltages for Fe-Ga and Fe-Ni wire sensors are 51.5mV and 36.5mV, respectively, and the output voltage of Fe-Ga wire sensor is obviously higher than that of Fe-Ni wire sensor under the same magnetic field. The model can be used to predict the output voltage of the sensor and to provide guidance for the optimization design of the sensor. © 2017 Author(s). All article content, except where otherwise noted, is licensed under a Creative Commons Attribution (CC BY) license (<http://creativecommons.org/licenses/by/4.0/>). <https://doi.org/10.1063/1.5006418>

## I. INTRODUCTION

Magnetostrictive displacement sensor has the advantages of high measuring accuracy, large measuring range and high reliability. It is widely used in the field of displacement control and petrochemical level measurement.<sup>1-4</sup> The signal generation mechanism of magnetostrictive displacement sensor has been deeply studied and the signal of sensor arises from the free rotation of magnetic domains and the wave effects of magnetic source.<sup>5</sup> Li et al. have found that magnetostriction of the waveguide wire is an important factor for the Wiedemann effect, and that the Wiedemann torsion increases with magnetostriction.<sup>6</sup> The signal amplitude of Fe-Ga waveguide wire displacement sensor is higher than that of Fe-Ni waveguide wire displacement sensor.<sup>7</sup> In the previous work, the output voltage model of magnetostrictive displacement sensor under the action of spiral magnetic field was established.<sup>8</sup> However, the output voltage model does not determine the relation between the output characteristics of sensor and the magnetostriction of waveguide wire. In fact, the Wiedemann twist angle produced by the waveguide wire is related to the magnetostriction of the waveguide wire.<sup>6,9</sup> Therefore, it is interesting to investigate the relationship between the output voltage of magnetostrictive displacement sensor and the magnetostriction of the waveguide.

## II. STRUCTURE AND OUTPUT VOLTAGE MODEL OF SENSOR

The displacement sensor is mainly composed of waveguide wire, permanent magnet, detecting coil, damper, and its structure is shown in Fig. 1. The axial bias magnetic field,  $H_b$ , is generated

<sup>a</sup>Corresponding Author is Li Yuanyuan. Electronic mail: [201621401033@stu.hebut.edu.cn](mailto:201621401033@stu.hebut.edu.cn).

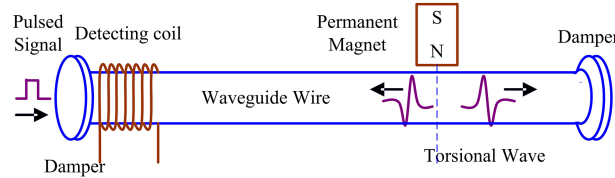


FIG. 1. The structure diagram of magnetostrictive displacement sensor.

by the permanent magnets and the circumferential excitation magnetic field,  $H_d(r)$ , is generated by the pulse current, which flows through the guide wire. The axial magnetic field and the excitation magnetic field are superposed together to produce a torsional magnetic field,  $H(r)$ , at an angle of  $\theta$  to the axial direction of the waveguide wire.<sup>8</sup>

Under  $H(r)$ , the magnetic moment of the waveguide wire turns toward the direction of  $H(r)$ . Then, the waveguide wire produces a torsional magnetostrictive strain along  $H(r)$ . The torsional magnetostrictive effect is also known as the Wiedemann effect. The domain of the waveguide wire produces local deflection under the strong dynamic load, and the vibration of the domains results in the generation of stress waves. Due to the inverse magnetostrictive effect, when the torsional wave reaches the detection coil, the mechanical stress leads to the change of the magnetic induction intensity in the waveguide wire, so that the induced voltage can be detected by the detecting coil.<sup>5,9</sup> By testing the waveform of the voltage across the detecting coil, we can determine the time, from which the torsion wave is generated, and to which it is passed to the detecting coil, and measure the displacement.

The output voltage model of sensor can describe the dependence of the output voltage on the magnetostriction and magnetic field. According to Faraday's law, the induced electromotive force,  $e$ , can be expressed as follows:

$$e = -N \frac{d\phi}{dt} = -NS \frac{dB}{dt} \quad (1)$$

where  $N$  is the detecting coil turns,  $S$  is the cross-sectional area,  $\phi$  is the magnetic flux,  $B$  is the magnetic-induced intensity in the waveguide wire and  $t$  is the time. According to the conversion relation between the mechanical energy and magnetic field energy in the waveguide wire,<sup>10,11</sup>  $B$  can be described as

$$B = 4\pi\lambda\mu \frac{\partial\varphi}{\partial x} \quad (2)$$

where  $\mu = \mu_r\mu_0$  is the absolute permeability of waveguide wire,  $\partial\varphi/\partial x$  is the angular strain, and  $\lambda$  is the rate of magnetic field change caused by angular strain, which can be determined by the experimental method. In Refs.8,  $\partial\varphi/\partial x = T/GI_a$ , among which  $T$  is torque,  $G$  is the shear modulus of the material,  $I_a$  is the polar moment of inertia of the cross section of the waveguide wire, the solution of the angular strain is converted into the solution of the torque.<sup>8</sup>

The waveguide wire covered by the permanent magnet is axially divided into a plurality of cylinders, each of which represents a unit body, as shown in Fig. 2. Here  $d\varphi$  is the relative torsional angle of the cross section of the cylinder,  $dx$  is the length of the element,  $R$  is the radius of a cylinder, then the shear strain can be approximately expressed as

$$\gamma \approx \frac{Rd\varphi}{dx} \quad (3)$$

By analyzing the thin cylinder,  $d\gamma$  obtained as follows<sup>12</sup>

$$d\gamma = 2(\lambda_l - \lambda_t) \sin\theta \cos\theta \quad (4)$$

where  $\lambda_l$  and  $\lambda_t$  are the axial and transverse magnetostriction of the wire, respectively.

Since the direction of  $H_b$  is perpendicular to that of  $H_d(r)$ , there are the relations  $\sin\theta = H_d(r)/\sqrt{(H_b)^2 + H_d(r)^2}$  and  $\cos\theta = H_b/\sqrt{(H_b)^2 + H_d(r)^2}$ . The wave velocity is  $v_0 = \sqrt{G/\rho}$ ,  $G = E/2(1+\nu)$ , where  $G$  is the modulus of rigidity,  $\rho$  is the density of the wire,  $E$  is the Young's modulus,  $\nu$  is the Poisson's ratio, the length of the detecting coil can be expressed as  $L_n = v_0 t$ ,

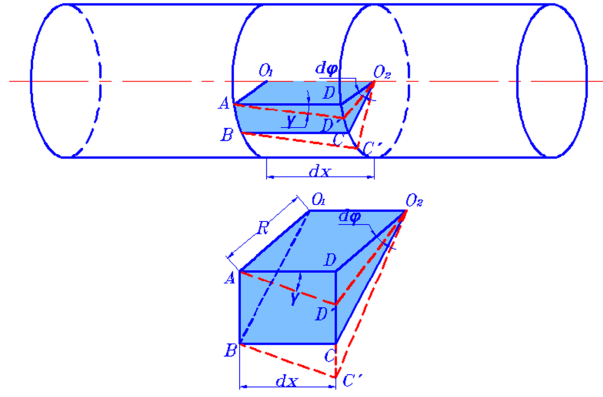


FIG. 2. Torsion diagram of waveguide wire element.

where  $t$  is the time that the stress wave passes through the test coil, so the shear strain can be expressed as:

$$\gamma = 2(\lambda_l - \lambda_t) L_n \frac{H_b H_d(r)}{H_b^2 + H_d(r)^2} \quad (5)$$

According to Equations (3–5), the twist angle<sup>6,9</sup> per unit length can be written as

$$\frac{d\varphi}{dx} = \frac{2(\lambda_l - \lambda_t) L_n}{R} \frac{H_b H_d(r)}{H_b^2 + H_d(r)^2} \quad (6)$$

The magnitude of the output voltage depends on the degree of torsional deformation of the waveguide wire covered by the detecting coil. According to Equations (1), (2), (6), the output voltage can be written as

$$e = \frac{8\pi\lambda\mu NS(\lambda_l - \lambda_t) \sqrt{\frac{E}{2(1+\nu)\rho}}}{R} \frac{H_b H_d(r)}{H_b^2 + H_d(r)^2} \quad (7)$$

In the equation (7), the magnetic field and the magnetostriction of waveguide wire are variables. In addition, the magnetostrictive displacement sensor model includes some parameters that relate to the detecting coil and waveguide wire material. The four variables,  $H_b$ ,  $H_d(r)$ ,  $\lambda_l$  and  $\lambda_t$  are the most important factors that affect the sensor output characteristic. In the equation (7), the output voltage of the displacement sensor linearly increases with the difference between the axial and transverse magnetostriction of the waveguide wire. Compared with the output voltage model established by Refs.8 and 10, the model in this paper has clearly determined the relation between the output voltage of magnetostrictive displacement sensor and the magnetostriction of waveguide wire. In fact, the magnetostrictive difference accurately reflects the magnetostrictive strain of the waveguide wire and describes the contribution of magnetostrictive strain to the torsional angle.

### III. RESULTS AND ANALYSIS

When  $H_b = 9.28$  kA/m and  $H_d$  is 3.4 kA/m, 3.82 kA/m and 4.25 kA/m, respectively, the output voltage of the displacement sensor is calculated by using the equation (7), as shown in Fig. 3(a) (lines). The detecting coil turns  $N = 800$ , the cross-sectional area of detecting coil  $S = 15.89$  mm<sup>2</sup>.  $R = 0.25$  mm,  $E = 57$  MPa,  $\rho = 7.6$  g/cm<sup>3</sup>,  $\nu = 0.2$ ,  $\mu_r = 85$  for Fe<sub>83</sub>Ga<sub>17</sub> wire.<sup>10,13,14</sup>  $R = 0.25$  mm,  $E = 180$  MPa,  $\rho = 8.0$  g/cm<sup>3</sup>,  $\nu = 0.25$ ,  $\mu_r = 200$  for Fe<sub>40</sub>Ni<sub>60</sub> wire.<sup>10,14</sup>  $\lambda = 0.0784$  A/m according to the experiment. As the frequency of the pulse current is very high, the skin effect causes the exciting magnetic field to be concentrated in the waveguide wire surface. Therefore, using the waveguide wire surface excitation magnetic field,  $H_d(R)$ , instead of  $H_d(r)$ .

From Fig. 3(a), the output voltage is linearly related to the magnetostrictive difference,  $(\lambda_l - \lambda_t)$ . When  $(\lambda_l - \lambda_t)$  is small, the corresponding torsional strain becomes small, the magnetostrictive effect

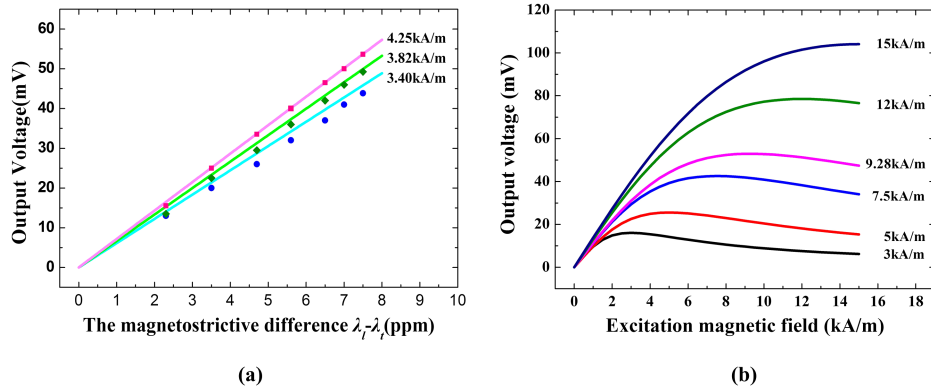


FIG. 3. (a) The magnetostrictive difference dependence of output voltage under different  $H_d$  (b) The excitation magnetic field dependence of output voltage under different  $H_b$ .

is not obvious, and the output voltage detected by the coil is also small. When  $(\lambda_I - \lambda_t)$  is large, the output voltage becomes large. When  $(\lambda_I - \lambda_t)$  is in the range of 0 to 8 ppm, the value of output voltage changes in the range of 0 to 57.3 mV.

The output voltage has been measured and the relation between it and the magnetostrictive difference is also shown in Fig. 3(a) (experimental dots). A TFG6920A signal generator was used to generate the excitation pulse current of 1 kHz, width of 7  $\mu$ s, and high level 5 V. From Fig. 3(a), the experimental result is consistent with calculating one. It is obvious that the magnetostrictive difference has a great influence on the output voltage. In order to obtain larger output voltage, the alloy wire with the larger magnetostrictive difference should be chosen.

The calculating curve of the output voltage with the excitation fields under different bias magnetic field is shown in Fig. 3(b). The output voltage increases with increasing  $H_d$ , when  $H_d < 3$  kA/m and  $H_b = 3$  kA/m, and it gradually decreases when  $H_d > 3$  kA/m and  $H_b = 3$  kA/m. The output voltage exhibits a peak when  $H_d = 3$  kA/m and  $H_b = 3$  kA/m. With increasing  $H_b$ ,  $H_d$ , corresponding to the voltage peak, increases. At the voltage peak,  $H_d$  nearly is equal to  $H_b$ . From the result in Fig. 3(b), the peak value of the output voltage increases with increasing  $H_b$ . When  $H_b = 15$  kA/m, the output voltage peak reaches 104 mV. It means that  $H_b$  should be enough high when a large output voltage of sensor is required.

The output voltages versus  $H_d$  for Fe-Ga and Fe-Ni waveguide wires at  $H_b = 9.28$  kA/m are presented in Fig. 4. From Fig. 4, the output voltage increases rapidly when  $H_d < 6$  kA/m, and increases slowly when  $H_d > 6$  kA/m. When  $H_d = 8$  kA/m, the measured output voltages for Fe-Ga and Fe-Ni wire sensors are 51.5 mV and 36.5 mV, respectively. It means that the output voltage of Fe-Ga wire sensor is obviously higher than that of Fe-Ni wire sensor under the same magnetic field. In fact, the

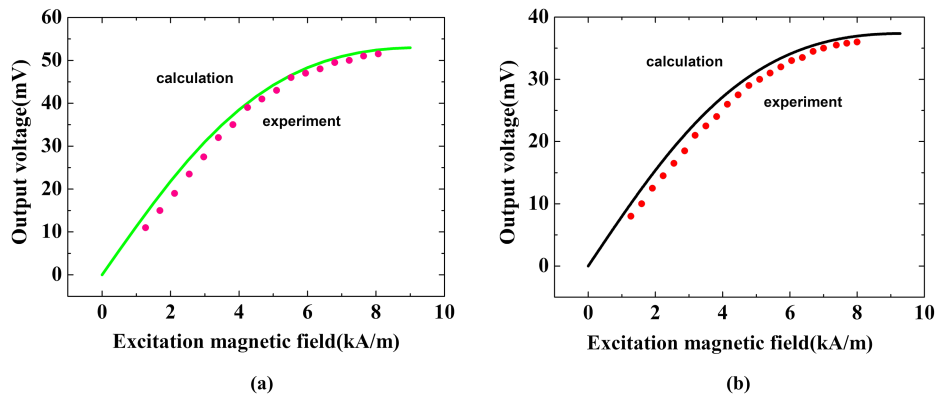


FIG. 4. The excitation magnetic field dependence of output voltage for the sensors. (a) Fe-Ga (b) Fe-Ni.

experimental measurement has shown that the magnetostriction of Fe-Ga wire is 5.6 ppm and that of Fe-Ni wire is 4 ppm when  $H_b = 9.28 \text{ kA/m}$ . The large magnetostriction of Fe-Ga wire makes the output voltage increase, compared with that of Fe-Ni wire sensor. From Fig. 4, the experimental result is basically consistent with the calculating one. The results indicate that the equation (7) can be used to describe the relation among the output voltage, magnetic field, and magnetostrictive difference. However, a small error exists between the experimental result and the calculating one, and it may be due to the substitution of  $H_d(R)$  for  $H_d(r)$ .

#### IV. CONCLUSIONS

The output voltage model of a magnetostrictive displacement sensor has been established according to the Wiedemann effect and inverse magnetostrictive effect. The calculating result is basically consistent with the experimental one, and the model can be used to describe the relation among the output voltage of the sensor, magnetic field, and magnetostrictive difference,  $(\lambda_l - \lambda_t)$ . A linear relationship exists between the output voltage and  $(\lambda_l - \lambda_t)$ . The larger  $(\lambda_l - \lambda_t)$  is, the greater the output voltage is. The measured output voltage for Fe-Ga wire sensor can reach 51.5 mV, when the bias magnetic field is 9.28 kA/m, and the excitation magnetic field is 8 kA/m. This result indicates that the magnetostrictive alloy wire should be with large magnetostrictive difference and that the bias magnetic field is in the range of 9 ~ 15 kA/m if a large output voltage is required.

#### ACKNOWLEDGMENTS

This work was supported by the National Natural Science Foundation of China (Grant No. 51777053), and the Natural Science Foundation of Hebei Province (No. E2017202035, E2014202246, E2016202034), and Jiangxi Province Key Laboratory of precision drive and control.

- <sup>1</sup> E. Hristoforou and R. E. Reilly, *IEEE Trans. Magn.* **30**(5), 2728 (1994).
- <sup>2</sup> E. Hristoforou, *Sens. Lett.* **7**(3), 303 (2009).
- <sup>3</sup> M. R. Karafi, Y. Hojjat, F. Sassani, and M. Ghodsi, *Sensor Actuators A Phys.* **195**(2), 71 (2013).
- <sup>4</sup> F. Martínez, I. Santiago, F. Sánchez, G. Obieta, A. García-Arribas, and J. M. Barandiarán, *J. Gutiérrez, Sensor Actuators A Phys.* **129**(1–2), 138 (2006).
- <sup>5</sup> C. Deng, Y. H. Kang, E. Li, Y. Zhang, J. Cheng, and T. Ge, *Meas.* **47**(1), 591 (2014).
- <sup>6</sup> J. Li, X. Gao, J. Zhu, X. Bao, L. Cheng, and J. Xie, *Chin. Phys.* **21**(8), 476 (2012).
- <sup>7</sup> M. Wun-Fogle, J. B. Restorff, and A. E. Clark, *IEEE Trans. Magn.* **42**(10), 3120 (2006).
- <sup>8</sup> L. Zhang, B. Wang, L. Weng, Y. Sun, and P. Wang, *Transactions of China Electrotechnical Society* **30**(12), 21 (2015).
- <sup>9</sup> X. Zhou, C. Yu, Z. Tang, C. Zhao, and H. Yan, *IEEE Sensors J.* **14**(1), 249 (2013).
- <sup>10</sup> L. Zhang, B. Wang, Y. Sun, L. Weng, and P. Wang, *IEEE Trans. Appl.* **26**(4), 1 (2016).
- <sup>11</sup> R. C. William, *IRE Transactions on Ultrasonic Engineering* **7**(1), 16 (2005).
- <sup>12</sup> E. Fromy, *Phys. J. Phys. Radium* **7**(1), 13 (1926).
- <sup>13</sup> J. Li, X. Gao, J. Xie, J. Zhu, X. Bao, and R. Yu, *Physica B* **407**(8), 1186 (2012).
- <sup>14</sup> L. Zhang, B. Wang, X. Yin, R. Zhao, L. Weng, Y. Sun, B. Cui, and W. Liu, *IEEE Trans. Magn.* **52**(7), 1 (2016).